



Cite this: DOI: 10.1039/d6dt00354k

# Coordination flexibility and function in tris(pyrazolyl)methanesulfonate coordination chemistry

Arantxa Forte-Castro, Juana M. Pérez and Ignacio Fernández \*

Tris(pyrazolyl)methanesulfonate (Tpms) ligands constitute water-compatible scorpionate platforms that combine the facial *N,N,N* donor set of classical tris(pyrazolyl)borates (Tp) or tris(pyrazolyl)methane (Tpm) with an appended sulfonate functionality that enhances hydrolytic robustness, solubility in polar media and coordination flexibility. Over the last two decades, Tpms chemistry has evolved from simple alkali-metal salts into structurally diverse complexes spanning much of the periodic table, in which the sulfonate group may remain non-coordinating or engage as an auxiliary, often hemilabile, donor. This donor complementarity enables  $\kappa^3/\kappa^2$  coordination switching, modulation of nuclearity, access to multinuclear and polymeric architectures, and fine control over metal-centre environments. In this Perspective, we critically analyse the emerging structure–property relationships that govern Tpms coordination modes, stability and dimensionality and assess how these features translate into enabling functions in oxidation and carbonylation catalysis, Lewis-acid-mediated C–C bond formation, biologically active silver and copper systems, and coordination polymer design. Finally, we outline key challenges and opportunities for the field, including rational ligand-design strategies to control sulfonate engagement, the need for mechanistic benchmarking under aqueous and green conditions, and the potential of Tpms ligands as general scaffolds for sustainable and functional inorganic chemistry.

Received 10th February 2026,  
Accepted 26th March 2026

DOI: 10.1039/d6dt00354k

rsc.li/dalton

## 1. Introduction

The development of tridentate nitrogen-donor ligands has become a central theme in coordination and organometallic chemistry, driven by their well-defined coordination modes and broad applicability in catalysis, materials science and bioinorganic modelling. Among these systems, scorpionate ligands—most notably tris(pyrazolyl)borates (Tp)—have achieved particular prominence owing to their facial tripod coordination and the possibility of fine-tuning steric and electronic properties through pyrazole substitution.<sup>1–3</sup> Since their introduction by Trofimenko,<sup>4</sup> poly(pyrazolyl)borate ligands have evolved into a highly versatile class of scorpionate systems. A key feature of Tp ligands is the possibility to systematically tune their steric and electronic properties through substitution at the 3-, 4- and 5-positions of the pyrazolyl rings. Such modifications enable fine control over metal–ligand interactions, coordination number and geometry, ranging from classical  $\kappa^3$ -*N,N,N* facial binding to reduced  $\kappa^2$  coordination modes or distorted geometries under steric constraints (Fig. 1).<sup>5–7</sup> As a result, Tp has become one of the most widely employed tripod ligand platforms, finding applications in areas such as bioinorganic modelling—where it mimics histidine-rich coordination environ-

ments—as well as in homogeneous catalysis, metal extraction and biomimetic chemistry.<sup>2,8–15</sup> Despite these successes, the use of many Tp complexes in polar or aqueous media can be limited by their low water solubility and, in some cases, by their susceptibility to hydrolytic degradation. These features have motivated the search for related ligand platforms better suited to such environments.<sup>2,16,17</sup>

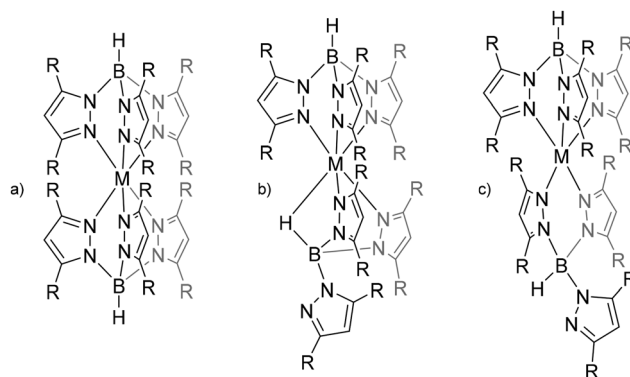


**Fig. 1** Representative steric and coordination diversity of tris(pyrazolyl) borate (Tp) ligands. Substituents (R) on the pyrazolyl rings modulate steric demand and enable different coordination modes, including (a) classical  $\kappa^3$ -*N,N,N* facial binding, (b)  $\kappa^2$  coordination with secondary M...H–B interactions, and (c) reduced coordination environments under increased steric constraints.

Department of Chemistry and Physics, Research Centre CIAIMBITAL, University of Almería, Ctra. Sacramento s/n, 04120 Almería, Spain. E-mail: ifernan@ual.es



An isoelectronic and isosteric alternative to Tp is tris(pyrazolyl)methane (Tpm), which preserves the facial tridentate binding motif while offering greater synthetic flexibility. Substitution at the pyrazole rings enables straightforward access to a wide range of derivatives, allowing steric and electronic modulation without altering the tripodal framework.<sup>2,6,18,19</sup> Building on this scaffold, Kläui and co-workers introduced the sulfonated analogue tris(pyrazolyl)methanesulfonate (Tpms),<sup>20</sup> obtained by replacing the methine proton of Tpm with a methanesulfonate group (Fig. 2).

The incorporation of a sulfonate functionality endows Tpms ligands with several key advantages over classical scorpionates. These include enhanced resistance to hydrolysis, excellent solubility in polar solvents (including water), and remarkable stability across a wide pH range in aqueous media. Beyond these physicochemical benefits, the sulfonate unit introduces an additional anionic donor site that can remain non-coordinating or participate directly in metal binding, thereby expanding the accessible coordination space.<sup>20–22</sup> As a result, Tpms retains the monoanionic, formally  $C_{3v}$ -symmetric  $N$ -donor character of Tp, while the replacement of the B–H fragment with a sulfonate-bearing carbon centre generates a chemically robust yet functionally versatile ligand platform.<sup>6,23</sup>

Although the early development of Tpms chemistry was previously surveyed by Martins and co-workers in 2016,<sup>24</sup> the significant growth of the field over the last decade warrants a new perspective. These features have positioned Tpms as an attractive alternative to traditional scorpionate ligands, stimulating growing interest in its coordination and organometallic chemistry. Rather than providing an exhaustive catalogue of reported compounds, this Perspective offers a critical analysis of how the distinctive structural elements of Tpms, particularly sulfonate incorporation and coordination flexibility, govern metal binding, reactivity and function, and how these attributes can be exploited in catalysis, biologically relevant systems and functional materials.

## 2. Tris(pyrazolyl)methanesulfonate ligands

### 2.1. Synthesis and general features

Tris(pyrazol-1-yl)methanesulfonate (Tpms,  $C(pz)_3SO_3^-$ ) ligands constitute a family of stable and versatile scorpionate-type donors that are both isoelectronic and isosteric with clas-

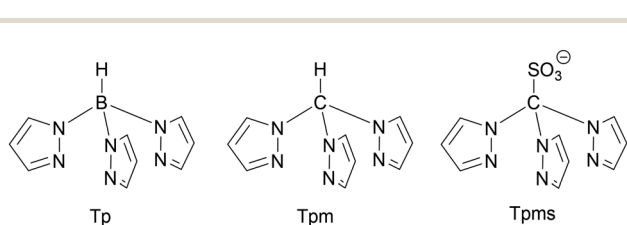


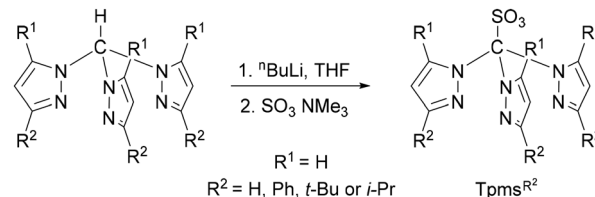
**Fig. 2** Comparison of classical scorpionate ligands tris(pyrazolyl)borate (Tp) and tris(pyrazolyl)methane (Tpm) with the sulfonated analogue tris(pyrazolyl)methanesulfonate (Tpms), highlighting the replacement of the B–H or C–H unit with a methanesulfonate functionality in Tpms.

sical tris(pyrazolyl)borates (Tp). As in Tp systems, the pyrazolyl rings impart high chemical robustness, including resistance to oxidative and reductive conditions, while substitution at the pyrazole framework enables fine modulation of steric and electronic properties.<sup>22,25–29</sup> A defining distinction, however, arises from the replacement of the B–H unit with a sulfonate-bearing carbon centre, which profoundly alters solubility, hydrolytic stability and coordination behaviour. The prototypical lithium salt, LiTpms, was first reported by Kläui in 2000 *via* deprotonation of tris(pyrazolyl)methane in THF with *n*-butyllithium, followed by sulfonation using a sulfur trioxide–trimethylamine adduct and crystallisation from hot methanol.<sup>20</sup> This modular and operationally simple route provides direct access to Tpms and related derivatives in good yields and has become the standard synthetic entry point for this ligand class (Scheme 1). Importantly, the resulting salts display excellent solubility in polar solvents, including water, setting Tpms apart from many classical scorpionate systems and enabling downstream chemistry under aqueous or protic conditions.

### 2.2. Structural variations and steric control

Beyond the parent Tpms framework, the introduction of sterically demanding substituents at the 3-position of the pyrazolyl rings has given rise to so-called “second-generation” Tpms ligands.<sup>23,30,31</sup> Representative examples include Tpms<sup>Ph</sup>, Tpms<sup>iPr</sup> and Tpms<sup>tBu</sup>, which provide a systematic means to modulate the steric environment around the metal centre without disrupting the tripodal scaffold.

The phenyl-substituted derivative Tpms<sup>Ph</sup> was prepared by Wanke and co-workers through low-temperature deprotonation of Tpm<sup>Ph</sup> followed by sulfonation with  $SO_3 \cdot NMe_3$ .<sup>29</sup> Notably, the resulting lithium salt retains high solubility in polar media (MeOH, EtOH, acetone, and water), illustrating how the sulfonate functionality compensates for the increased hydrophobicity introduced by bulky aryl substituents. Analogous synthetic strategies afford Tpms<sup>iPr</sup> and Tpms<sup>tBu</sup>, whose steric bulk effectively suppresses the formation of multinuclear “sandwich-type” assemblies commonly encountered with less hindered scorpionate ligands.<sup>22,23,26,32</sup> Collectively, these derivatives establish steric encumbrance as a powerful design parameter in Tpms chemistry, allowing control over nuclearity, coordination number and accessibility of the metal centre while pre-



**Scheme 1** General synthetic route to tris(pyrazolyl)methanesulfonate (Tpms) ligands *via* deprotonation of tris(pyrazolyl)methane derivatives, followed by sulfonation with the  $SO_3 \cdot NMe_3$  adduct, illustrating access to the parent Tpms ligand ( $R^1 = H$ ) and sterically modified second-generation derivatives ( $R^1 = H, Ph, i\text{-Pr}$  or  $t\text{-Bu}$ ).



servicing the favourable solubility and stability imparted by the sulfonate group (Scheme 1).

### 2.3. Coordination flexibility and sulfonate engagement

Tpms ligands and their derivatives share with Tp ligands their monoanionic,  $C_{3v}$ -symmetric, tripodal nature, but the replacement of the B-H moiety with a methanesulfonate group introduces additional donor flexibility. This modification confers significant coordination versatility, allowing Tpms ligands to function either as tripodal or bipodal donors.<sup>6</sup> Crystallographic and spectroscopic data reveal that Tpms ligands can adopt multiple coordination modes, including  $\kappa^3$ - $N,N,N$  binding through the three pyrazolyl nitrogen atoms (a),  $\kappa^3$ - $N,N,O$  coordination involving two pyrazolyl nitrogens and one sulfonate oxygen (b),  $\kappa^2$ - $N,N$  coordination through two pyrazolyl rings (c), and  $\kappa^2$ - $N,O$  binding with one pyrazolyl nitrogen and one sulfonate oxygen (d).<sup>30,32</sup> This adaptability enables reversible  $\kappa^3/\kappa^2$  switching and facilitates access to multinuclear and polymeric architectures (Fig. 3).

Infrared spectroscopy has proven particularly diagnostic for assessing sulfonate involvement in coordination. For Tpms salts in which the sulfonate group remains non-coordinating, two characteristic  $SO_3$  stretching bands are typically observed, consistent with retained  $C_{3v}$  symmetry: the asymmetric stretching mode  $\nu_{as}(SO_3)$  appears around 1220–1240  $cm^{-1}$ , while the symmetric mode  $\nu_s(SO_3)$  is found in the 1055–1070  $cm^{-1}$  region.<sup>27</sup> In contrast, coordination of the sulfonate oxygen lowers the local symmetry to  $C_s$ , leading to splitting of the  $SO_2$ -related stretching modes into three distinct bands, typically observed at 1285–1315  $cm^{-1}$  [ $\nu_{as}(SO_2)$ ], 1185–1205  $cm^{-1}$  [ $\nu_s(SO_2)$ ], and 1030–1040  $cm^{-1}$  [ $\nu(S-O)$ ].

The transition from two to three bands therefore provides a clear spectroscopic signature of sulfonate coordination. These trends correlate closely with solid-state structures and can also

be used to probe coordination equilibria in solution. For example, the potassium salt  $KTpms^{tBu}$  displays the two-band pattern expected for a non-coordinating sulfonate group, whereas  $LiTpms^{tBu}$  and  $TiTpms^{tBu}$  exhibit the three-band pattern associated with sulfonate coordination.<sup>20,27</sup>

In transition-metal complexes, analogous behaviour is observed: zinc halide species  $[(Tpms^{tBu})ZnX]$  ( $X = Cl, Br$ ) show spectroscopic features consistent with  $\kappa^3$ - $N,N,O$  coordination, while nickel analogues  $[(Tpms^{tBu})NiX]$  retain  $\kappa^3$ - $N,N,N$  binding with a non-coordinating sulfonate group.<sup>22</sup> Differences in  $SO_2$  band positions and relative intensities, together with changes in pyrazolyl vibrations, further allow semi-quantitative assessment of sulfonate engagement under different conditions. Taken together, these studies reveal the sulfonate group as a switchable auxiliary donor that responds sensitively to metal identity and coordination environment. This combination of enhanced solubility, hydrolytic stability and tunable donor behaviour positions Tpms ligands as versatile scorpionate platforms whose coordination chemistry not only parallels that of Tp, but in many respects extends it. These features underpin the diverse reactivity and functional applications discussed in the following sections.

## 3. Metal complexes of tris(pyrazolyl)methanesulfonate across the periodic table

Although Tpms coordination chemistry is less extensive than that of classical tris(pyrazolyl)borates, the available studies already reveal distinctive, recurring patterns that are specific to sulfonated scorpionates. In the following sections, we therefore adopt a concept-driven view, focusing on how sulfonate incorporation reshapes solubility, coordination mode preferences and nuclearity, and how these features enable redox/oxo chemistry, organometallic reactivity and extended architectures. The discussion highlights representative systems and the design rules they suggest, rather than providing an exhaustive catalogue of reported complexes.

### 3.1. Salt platforms and pre-coordination behaviour: alkali metals and Tl(I)

Alkali-metal and thallium(I) Tpms derivatives define the baseline coordination behaviour of sulfonated scorpionates in the absence of strong d-block metal preferences. These systems illustrate how the sulfonate group can remain non-coordinating, engage in O-only binding modes, or promote oligomeric assemblies, thereby establishing reference points for interpreting sulfonate engagement in transition-metal complexes. The lithium salt  $LiTpms$  and its sterically modified congeners are readily accessed by metathesis reactions and typically display higher degrees of sulfonate engagement than their heavier alkali-metal analogues. Infrared spectroscopic studies provide a clear diagnostic of this behaviour:  $LiTpms^{tBu}$  exhibits three  $\nu(SO_3)$  bands characteristic of reduced symmetry and sulfonate

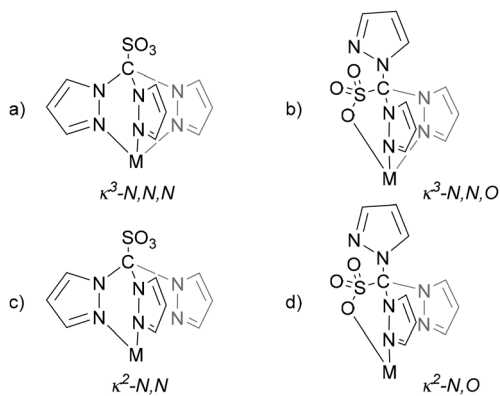


**Fig. 3** Representative coordination modes of tris(pyrazolyl)methanesulfonate (Tpms) ligands: (a)  $\kappa^3$ - $N,N,N$  coordination through the three pyrazolyl nitrogen atoms; (b)  $\kappa^3$ - $N,N,O$  coordination involving two pyrazolyl nitrogens and one sulfonate oxygen; (c)  $\kappa^2$ - $N,N$  coordination with one pyrazolyl arm unbound; and (d)  $\kappa^2$ - $N,O$  coordination featuring one pyrazolyl nitrogen and one sulfonate oxygen. The ability of the sulfonate group to remain non-coordinating or to engage as an auxiliary donor underpins the coordination flexibility of Tpms ligands.



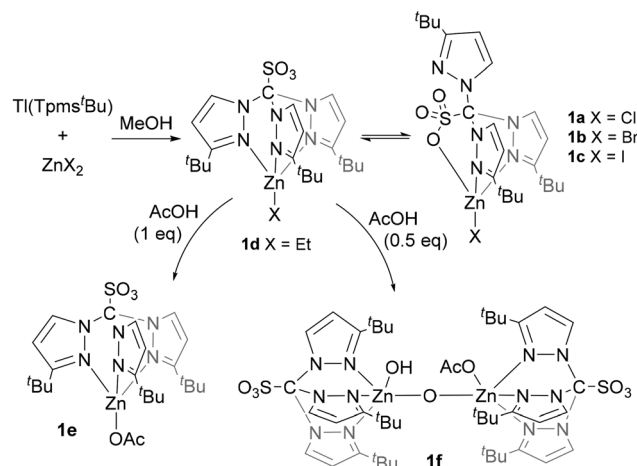
coordination, whereas the potassium analogue  $\text{KTpms}^{\text{tBu}}$  shows only two  $\nu(\text{SO}_3)$  bands, consistent with retention of  $C_{3v}$  symmetry and a non-coordinating sulfonate group.<sup>20,27</sup> These observations highlight the sensitivity of sulfonate binding to cation size and Lewis acidity, even in the absence of d-orbital participation. In the solid state,  $\text{LiTpms}$  derivatives can crystallise as monomeric or oligomeric assemblies, where the sulfonate group may remain a spectator or engage in  $\kappa^2\text{-O,O}$  interactions that link metal centres into higher-order structures.<sup>32</sup> Such behaviour illustrates the propensity of the sulfonate moiety to act as a structural organiser under favourable electrostatic conditions, foreshadowing its role in coordination polymers and multinuclear transition-metal systems. The post-transition-metal thallium(i) derivative  $\text{TlTpms}^{\text{tBu}}$  represents a limiting case in which  $\text{Tpms}$  coordination is dominated exclusively by the sulfonate functionality. Structural and spectroscopic studies reveal  $\text{O}$ -only binding of the ligand, with no involvement of the pyrazolyl nitrogen donors.<sup>20,27</sup> This behaviour contrasts sharply with that observed for d-block metals and underscores the capacity of  $\text{Tpms}$  to adapt its donor set in response to metal softness and coordination preferences.

Collectively, alkali-metal and  $\text{Tl}(i)$   $\text{Tpms}$  salts establish key reference points for understanding sulfonate engagement, coordination flexibility and aggregation tendencies. These systems define the baseline against which metal-driven coordination switching, redox chemistry and structural diversification in transition-metal complexes can be meaningfully interpreted.

### 3.2. When the sulfonate competes: coordination-mode switching and auxiliary donor behaviour

One of the defining features of  $\text{Tpms}$  ligands is the ability of the sulfonate group to compete with pyrazolyl nitrogen donors for metal coordination. This section examines metal-dependent  $\kappa^3/\kappa^2$  switching and  $N,N,N$  versus  $N,N,O$  binding motifs (Fig. 3), highlighting cases where subtle changes in metal identity, oxidation state or coordination environment determine whether the sulfonate remains a spectator or becomes an active donor. Comparisons across transition-metal series reveal how sulfonate engagement can be harnessed to modulate geometry, nuclearity and solution dynamics. Early evidence of sulfonate competition can be identified by comparison across closely related metal systems. In zinc(ii) halide complexes  $[(\text{Tpms}^{\text{tBu}})\text{ZnX}]$  ( $X = \text{Cl}, \text{Br}, \text{I}$ ) (**1a–c**), solid-state structures reveal  $\kappa^3\text{-N,N,O}$  coordination, with the sulfonate oxygen completing a distorted tetrahedral environment around zinc (Scheme 2).<sup>22</sup>

$^1\text{H}$  NMR studies in  $\text{CDCl}_3$  reveal distinctive solution behaviour: while the chloride and bromide analogues exhibit three sets of pyrazolyl resonances in a 1 : 2 intensity ratio, consistent with a solution equilibrium between a  $C_{3v}$ -symmetric species and a  $C_s$ -symmetric isomer, the iodide derivative displays exclusively the  $C_s$ -symmetric form even at low temperature. This trend highlights the subtle interplay between halide identity, metal Lewis acidity and sulfonate engagement. Further insight into sulfonate-assisted coordination flexibility is pro-

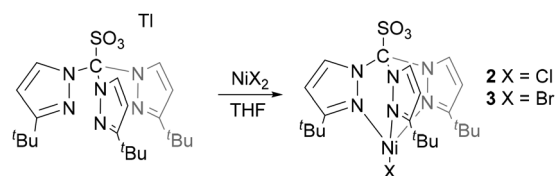


**Scheme 2** Zinc(ii) complexes supported by the sulfonated scorpionate ligand  $\text{Tpms}^{\text{tBu}}$ , illustrating sulfonate-assisted coordination flexibility. Solid-state  $\kappa^3\text{-N,N,O}$  coordination is observed for the halide derivatives  $[(\text{Tpms}^{\text{tBu}})\text{ZnX}]$  ( $X = \text{Cl}, \text{Br}, \text{I}$ ), while subsequent alkylation and protonolysis reactions afford the monoacetate complex  $[(\text{Tpms}^{\text{tBu}})\text{ZnOAc}]$  or a dinuclear species featuring asymmetric bridging units, depending on the reaction conditions.

vided by the reactivity of these zinc systems. Treatment of  $\text{Tl}(\text{Tpms}^{\text{tBu}})$  with diethylzinc in THF affords the alkyl complex  $[(\text{Tpms}^{\text{tBu}})\text{ZnEt}]$  (**1d**), which upon reaction with acetic acid yields either the monoacetate derivative  $[(\text{Tpms}^{\text{tBu}})\text{ZnOAc}]$  (**1e**) or a dinuclear species, depending on the number of equivalents of acetic acid employed.<sup>22</sup>

Infrared spectroscopy corroborates sulfonate engagement through the characteristic splitting of the  $\nu(\text{SO}_3)$  bands, while solution-phase NMR and IR studies indicate dynamic behaviour, involving partial sulfonate dissociation and interconversion toward  $\kappa^2\text{-N,N,N}$  binding. In contrast, the isostructural nickel(ii) analogues  $[(\text{Tpms}^{\text{tBu}})\text{NiX}]$  crystallise exclusively in  $\kappa^3\text{-N,N,N}$  coordination modes, with minimal spectroscopic evidence for sulfonate participation (Scheme 3).<sup>22</sup> This Zn/Ni divergence highlights how subtle differences in metal Lewis acidity and preferred coordination geometry govern sulfonate involvement. Notably, these nickel complexes represent the first reported Group 10  $\text{Tpms}$  derivatives, underscoring the structural robustness of bulky sulfonated scorpionate frameworks in stabilising tetrahedral  $\text{Ni}(ii)$  environments.

Cobalt(ii) chemistry provides further insight into sulfonate-assisted coordination expansion. The five-coordinate complex



**Scheme 3**  $[(\text{Tpms}^{\text{tBu}})\text{NiX}]$  ( $X = \text{Cl}, \text{Br}$ ) complexes showing  $\kappa^3\text{-N,N,N}$  coordination and a non-bonding sulfonate group, highlighting the metal-dependent nature of sulfonate participation in  $\text{Tpms}$  chemistry.

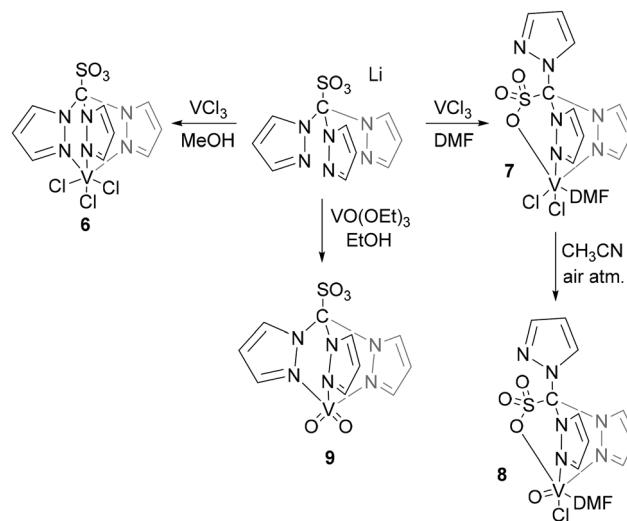


[[Tpms<sup>tBu</sup>CoCl(Hpz<sup>tBu</sup>)] (4) adopts a distorted trigonal–bipyramidal geometry in which the sulfonate oxygen occupies an axial position, stabilising a  $\kappa^3$ -*N,N,O* binding mode (Scheme 4a).<sup>22</sup> Despite its five-coordinate structure, the complex exhibits electronic features more commonly associated with four-coordinate Co(II) centres, underscoring the subtle yet significant electronic influence exerted by sulfonate coordination. In contrast, attempts to generate Tpms-supported Co(II) complexes under hydrolytic conditions can promote cleavage of the C(sp<sup>3</sup>)-S bond (Scheme 4b), yielding Tpm-based derivatives and sulfate-containing species.<sup>33</sup> Cyclic voltammetry of these products reveals an irreversible Co<sup>2+</sup>/Co<sup>+</sup> reduction process in the range -0.40 to -0.68 V vs. SCE (saturated calomel electrode), followed by oxidation waves at higher potentials (0.58–1.28 V). These results emphasise that sulfonate engagement, while generally reversible and hemilabile, may also enable alternative reaction pathways under specific chemical environments.

Vanadium systems further exemplify sulfonate competition in redox-active environments. While the V(IV) complex [VCl<sub>3</sub>(Tpms)] (6) adopts classical  $\kappa^3$ -*N,N,N* coordination,<sup>18,34</sup> oxovanadium derivatives such as (Tpms)VOCl(DMF) (8) exhibit *N,N,O* binding modes in the solid state, with spectroscopic evidence for equilibria between *N,N,N* and *N,N,O* coordination in solution (Scheme 5).<sup>35</sup>

Silva and co-workers subsequently reported the reaction of [VO(OEt)<sub>3</sub>] with LiTpms, affording the air-stable dioxovanadium(v) complex [VO<sub>2</sub>(Tpms)] (9) (Scheme 5).<sup>36</sup> This behaviour reflects the pronounced oxophilicity of vanadium and illustrates how sulfonate donors can be selectively recruited to stabilise high-valent and oxo-containing metal centres.

Taken together, these examples establish sulfonate competition as a tunable and predictable feature of Tpms coordination chemistry rather than a structural anomaly. Metal identity, oxidation state, steric environment and solvent collectively

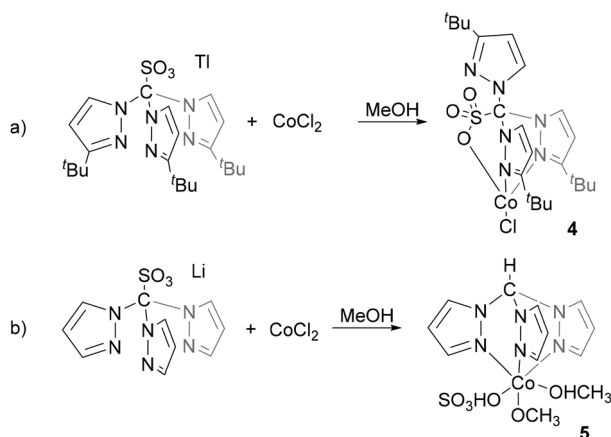


**Scheme 5** Vanadium complexes supported by tris(pyrazolyl)methane-sulfonate illustrating coordination-mode switching driven by oxidation state and oxo formation. While [VCl<sub>3</sub>(Tpms)] adopts  $\kappa^3$ -*N,N,N* coordination, oxovanadium derivatives display *N,N,O* binding involving the sulfonate oxygen, with solution equilibria between *N,N,N* and *N,N,O* modes.

determine whether the sulfonate group remains a spectator, acts as an auxiliary donor, or participates dynamically in coordination equilibria. This capacity for controlled donor switching distinguishes Tpms ligands from classical scorpionates and provides a powerful handle for modulating geometry, nuclearity and reactivity in downstream organometallic and catalytic applications.

### 3.3. Redox and oxo manifolds enabled by Tpms: early transition metals and high-valent species

Early transition metals provide a particularly revealing arena in which to assess the impact of sulfonated scorpionate ligands on redox chemistry and oxo formation. In this context, Tpms ligands combine two features that are rarely accessible simultaneously with classical scorpionates: (i) stabilisation of high oxidation states under polar conditions and (ii) the capacity of the sulfonate group to participate selectively in metal–oxo coordination environments. Vanadium, molybdenum and rhenium systems collectively illustrate how these attributes translate into structurally and electronically diverse redox manifolds. Vanadium chemistry offers the clearest illustration of oxidation-state-dependent behaviour. As discussed above, the V(IV) halide complex [VCl<sub>3</sub>(Tpms)] (6) adopts a conventional  $\kappa^3$ -*N,N,N* coordination mode and displays well-defined and reversible V(IV)/V(V) redox behaviour.<sup>18,34</sup> In contrast, oxovanadium derivatives formed either by aerial oxidation or controlled ligand substitution recruit the sulfonate oxygen into the coordination sphere, yielding *N,N,O*-bound species and solution equilibria between *N,N,N* and *N,N,O* binding modes (Scheme 5).<sup>35</sup> The dioxovanadium(v) complex [VO<sub>2</sub>(Tpms)] (9) extends this chemistry to higher oxidation



**Scheme 4** (a) [(Tpms<sup>tBu</sup>CoCl(Hpz<sup>tBu</sup>)] showing  $\kappa^3$ -*N,N,O* coordination and sulfonate-assisted stabilisation of a five-coordinate cobalt(II) centre. (b) Transformation of Tpms-supported cobalt complexes under protic conditions, illustrating ligand reorganisation and alternative coordination pathways.



states while reverting to a classical scorpionate binding mode, demonstrating that sulfonate engagement is not obligatory but is selectively triggered by oxophilicity and coordination demand.<sup>36</sup> Together, these systems establish Tpms as a ligand capable of accommodating redox-driven structural reorganisation without compromising stability in polar media.

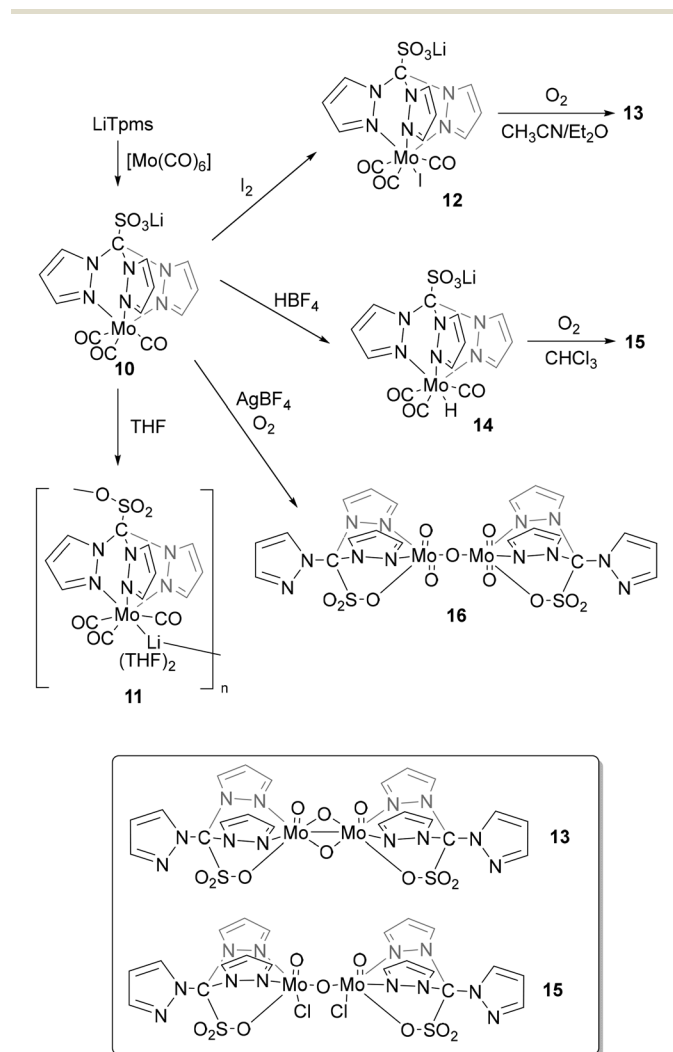
Molybdenum complexes further emphasise the versatility of Tpms in redox-active environments. Reaction of Li(Tpms) with  $[\text{Mo}(\text{CO})_6]$  affords the tricarbonyl species  $\text{Li}[\text{Mo}(\text{Tpms})(\text{CO})_3]$  (**10**), a rare example of a water-soluble molybdenum carbonyl complex.<sup>37</sup> This compound serves as a gateway to a rich redox landscape encompassing low- and high-valent molybdenum species (Scheme 6). Controlled oxidation, protonation or halide abstraction yields iodide, hydride and oxo derivatives, including Mo(v) and Mo(vi) oxo dimers in which the Tpms ligand adopts distinct coordination roles. Notably, the sulfo-

nate group may coordinate directly to the molybdenum centre or engage in secondary interactions with lithium ions to generate polymeric or supramolecular assemblies. These observations underscore the non-innocent nature of the sulfonate functionality, which contributes not only to solubility but also to structural diversification across oxidation states.

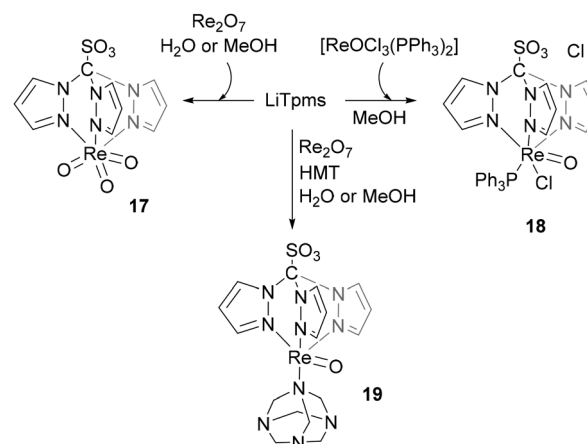
Rhenium chemistry provides a complementary perspective on high-valent oxo stabilisation. Tpms-supported rhenium(vii) oxo complexes such as  $[\text{ReO}_3(\text{Tpms})]$  (**17**) and mixed-ligand derivatives derived from  $\text{Re}_2\text{O}_7$  or  $[\text{ReOCl}_3(\text{PPh}_3)_2]$  illustrate the compatibility of Tpms ligands with strongly oxidising metal centres (Scheme 7).<sup>38</sup> These species retain structural integrity under aqueous or alcoholic conditions, highlighting the protective role of sulfonated scorpionates in harsh redox environments. Subsequent incorporation of neutral donors, as in  $[\text{ReO}(\text{Tpms})(\text{HMT})]$  (**19**), expands this chemistry to lower oxidation states and introduces electrochemically addressable Re(III)/Re(II) couples.<sup>28</sup> Cyclic voltammetry of this complex reveals a single-electron irreversible reduction wave, assigned to the  $\text{Re}(\text{III}) \rightarrow \text{Re}(\text{II})$  redox process.

Beyond discrete molecular complexes, Tpms ligands also enable the assembly of redox-active clusters. The  $[\text{VFe}_3\text{S}_4]^{2+}$  cubane-type clusters stabilised by Tpms represent an early and striking example of multimetallic architectures supported by sulfonated scorpionates (Scheme 8).<sup>39</sup> In these systems, the Tpms ligand contributes to both electronic modulation and solubility, allowing systematic variation of terminal ligands and fine-tuning of redox potentials without disruption of the metal-sulfur core.

Collectively, these early transition-metal systems demonstrate that Tpms ligands provide a robust yet adaptable platform for redox and oxo chemistry. Selective sulfonate recruitment, tolerance to high oxidation states and compatibility with polar and aqueous environments distinguish Tpms from classical scorpionates and underpin their growing relevance in oxidation catalysis and sustainable inorganic chemistry.

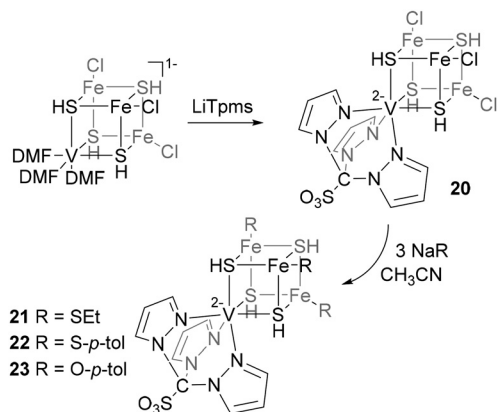


**Scheme 6** Redox- and ligand-induced transformations of the tricarbonyl complex  $\text{Li}[\text{Mo}(\text{Tpms})(\text{CO})_3]$ , providing access to low- and high-valent molybdenum species. Oxidation, protonation and halide abstraction afford iodide, hydride and oxo derivatives, including Mo(v) and Mo(vi) oxo dimers, highlighting the versatility of Tpms ligands in redox-active chemistry.



**Scheme 7** Tris(pyrazolyl)methanesulfonate-supported rhenium oxo complexes illustrating the stabilisation of high-valent Re(vii) species and their extension to lower oxidation states through coordination of neutral donor ligands.





**Scheme 8** Tpms-stabilised  $[VFe_3S_4]^{2+}$  clusters bearing different terminal ligands at the iron sites ( $Cl^-$ , thiolate and aryloxide). Variation of the terminal donor modulates the electronic properties of the cluster while preserving the metal–sulfur core.

### 3.4. Reactive organometallic motifs: carbonyl, hydride and small-molecule activation chemistry

Late transition metals supported by tris(pyrazolyl)methanesulfonate ligands exhibit a rich organometallic chemistry in which classical scorpionate coordination is combined with enhanced solubility, coordination adaptability and access to reactive intermediates. In contrast to the early transition-metal systems discussed above, where redox and oxo chemistry dominate, Tpms ligands in Groups 8 and 9 enable the stabilisation of carbonyl, hydride and coordinatively unsaturated species that are directly relevant to bond activation and catalysis.

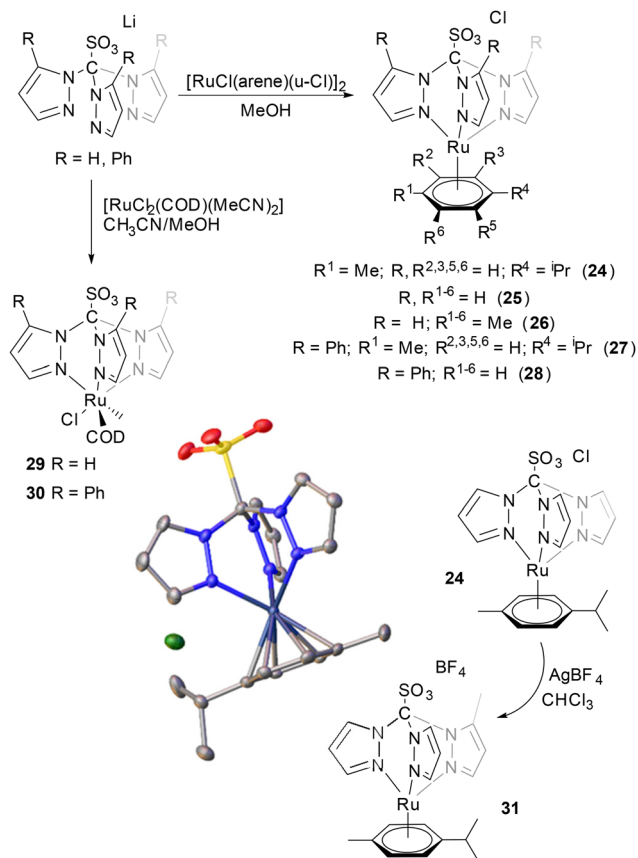
Ruthenium complexes constitute the most extensively developed family within this context. Half-sandwich species of the type  $[Ru(\eta^6\text{-arene})(Tpms)]Cl$  (**24–28**) and their phenyl-substituted analogues are readily obtained by reaction of  $Li(Tpms)$  or  $Li(Tpms^{Ph})$  with the corresponding chloro-bridged dimers and retain classical  $\kappa^3\text{-}N,N,N$  scorpionate binding (Scheme 9).<sup>23</sup>

These complexes are air-stable, soluble in polar solvents and serve as versatile precursors for further ligand substitution chemistry. Importantly, metathesis reactions and solvent-dependent rearrangements allow access to alternative coordination environments, including mixed donor sets and  $\kappa^3\text{-}N,N,O$  binding in specific cases.

Further diversification is achieved through phosphine coordination. The reaction of  $[RuCl_2(PPh_3)_3]$  with  $Li(Tpms)$  affords  $[RuCl\{Tpms\}(PPh_3)_2]$  (**32**), which displays solvent- and temperature-dependent coordination behaviour, undergoing reversible interconversion between  $\kappa^3\text{-}N,N,O$  and  $\kappa^3\text{-}N,N,N$  isomers (Scheme 10).<sup>21</sup>

Subsequent substitution with PTA gives rise to a family of well-defined  $\kappa^3\text{-}N,N,N$  complexes that can be further functionalised through electrophilic modification of the coordinated PTA ligand, providing a modular platform for post-synthetic diversification without disrupting the Tpms framework.

Hydride chemistry provides particularly compelling evidence of the ability of Tpms ligands to stabilise reactive inter-



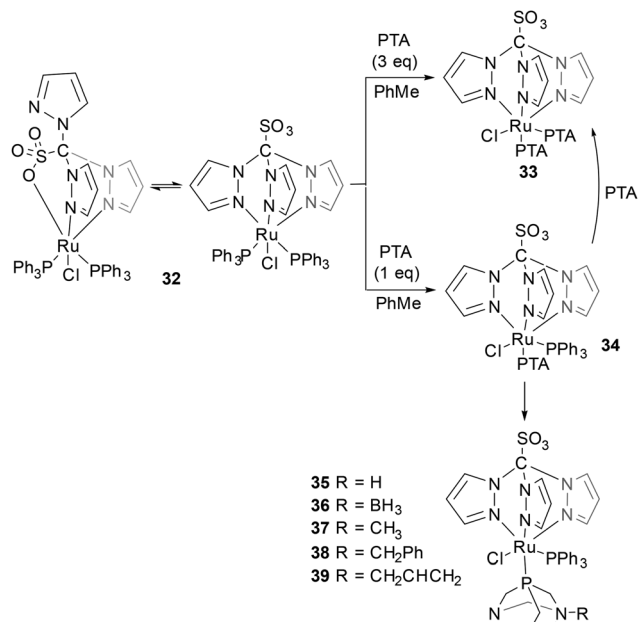
**Scheme 9** Synthesis of ruthenium(II) half-sandwich complexes supported by tris(pyrazolyl)methanesulfonate ligands. Reaction of  $Li(Tpms)$  or  $Li(Tpms^{Ph})$  with chloro-bridged arene ruthenium dimers affords  $[Ru(\eta^6\text{-arene})(Tpms)]Cl$  derivatives (arene = *p*-cymene, benzene or hexamethylbenzene), while reaction with  $[RuCl_2(COD)(CH_3CN)_2]$  provides access to  $Ru(COD)\text{-}Tpms$  complexes. The solid-state structure of complex **24**, shown with 50% probability ellipsoids, illustrates a representative coordination environment. Hydrogen atoms are omitted for clarity.

mediates. Reaction of  $[RuH_2(PPh_3)_4]$  with  $Li(Tpms)$  yields the monohydride  $[RuH(Tpms)(PPh_3)_2]$  (**40**), which undergoes protonation to form the molecular hydrogen complex  $[Ru(\eta^2\text{-}H_2)(Tpms)(PPh_3)_2]^+$  (**43**) (Scheme 11).<sup>40</sup> These species were unambiguously characterised by NMR spectroscopy, relaxation time measurements and isotopic labelling, representing rare examples of  $\eta^2\text{-}H_2$  complexes supported by sulfonated scorpionate ligands. This chemistry highlights the compatibility of Tpms frameworks with delicate metal–hydrogen bonding motifs.

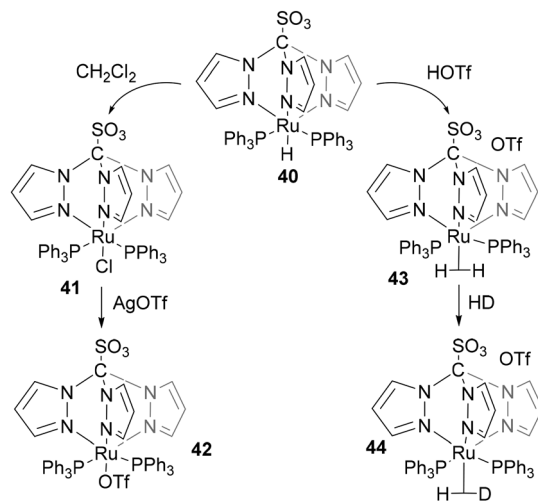
Iron chemistry provides an early entry point into Group 8 organometallic motifs supported by tris(pyrazolyl)methanesulfonate ligands. The first reported Tpms complex in this area was the iron(II) species  $Fe(Tpms)_2$  (**45**), synthesised by Gu in 2005.<sup>41</sup>

Subsequent derivatisation afforded the lithium salt  $Li_2[Fe(Tpms)(CN)_3]$  (**46**) that reacted with  $Mn(ClO_4)_2 \cdot 6H_2O$  in DMF to form a well-defined heterobimetallic compound,  $[Fe^{II}(Tpms)(CN)_3][Mn^{II}(H_2O)_2(DMF)_2] \cdot DMF$  (**47**) (Scheme 12). This trans-





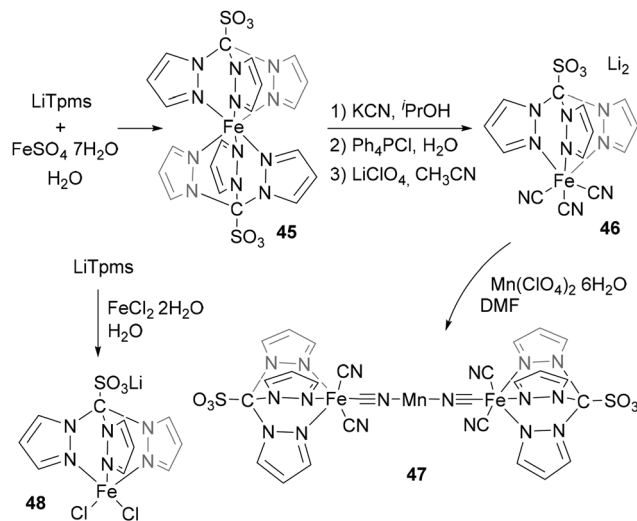
**Scheme 10** Solvent- and temperature-dependent coordination behaviour in ruthenium(II) tris(pyrazolyl)methanesulfonate complexes. Reaction of [RuCl<sub>2</sub>(PPh<sub>3</sub>)<sub>3</sub>] with Li(Tpms) affords [RuCl(Tpms)(PPh<sub>3</sub>)<sub>2</sub>], which undergoes reversible interconversion between κ<sup>3</sup>-N,N,O and κ<sup>3</sup>-N,N,N coordination modes. Subsequent substitution with PTA enables selective formation of κ<sup>3</sup>-N,N,N complexes and post-functionalisation at the coordinated phosphine.



**Scheme 11** Formation of Ru-hydride and η<sup>2</sup>-H<sub>2</sub> complexes supported by Tpms ligands, illustrating stabilisation of metal-hydrogen bonding motifs. Isotopic labelling experiments lead to the corresponding η<sup>2</sup>-HD species, confirming reversible H-H bond formation within the Tpms coordination environment.

formation highlights the capacity of Tpms-supported cyanometallates to engage in controlled secondary metal coordination.

In parallel, Silva and co-workers reported the pentacoordinate iron(II) complex Li[FeCl<sub>2</sub>(Tpms)] (**48**), obtained directly from FeCl<sub>2</sub>·2H<sub>2</sub>O and Li(Tpms) in water, which displays the

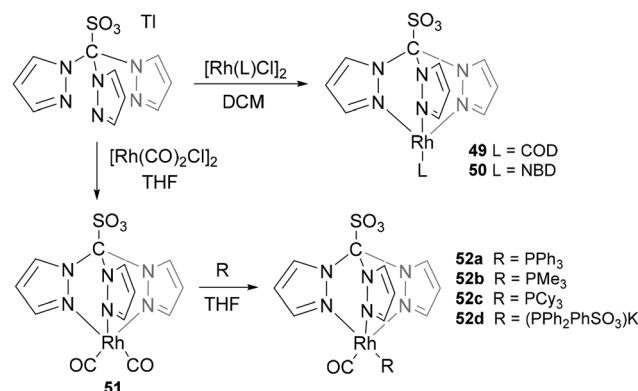


**Scheme 12** Iron(II) tris(pyrazolyl)methanesulfonate complexes illustrating early Group 8 organometallic motifs. Formation of [Fe(Tpms)<sub>2</sub>], its dilithiated derivative and the heterobimetallic {[Fe<sup>II</sup>(Tpms)(CN)<sub>3</sub>][Mn<sup>II</sup>(H<sub>2</sub>O)<sub>2</sub>(DMF)<sub>2</sub>]}·DMF assembly highlight the ability of Tpms-supported iron centres to engage in redox-active, multinuclear and secondary coordination chemistry, alongside classical κ<sup>3</sup>-N,N,N scorpionate binding in Li[FeCl<sub>2</sub>(Tpms)].

classical κ<sup>3</sup>-N,N,N scorpionate coordination mode (Scheme 12).<sup>18</sup>

Rhodium systems further demonstrate the potential of Tpms ligands in organometallic reactivity. Carbonyl and olefin complexes such as TpmsRh(COD) (**49**) (COD = 1,5-cyclooctadiene), TpmsRh(NBD) (**50**) (NBD = bicyclo[2.2.1]hepta-2,5-diene) and TpmsRh(CO)<sub>2</sub> (**51**) demonstrate flexible coordination behaviour, including κ<sup>3</sup>-N,N,N binding and bis-chelation modes depending on the ancillary ligands (Scheme 13).<sup>25,42</sup>

Photolysis of mixed carbonyl-phosphine derivatives generates coordinatively unsaturated Rh(I) species capable of activating aromatic C-H bonds.<sup>42</sup> Irradiation in benzene leads to

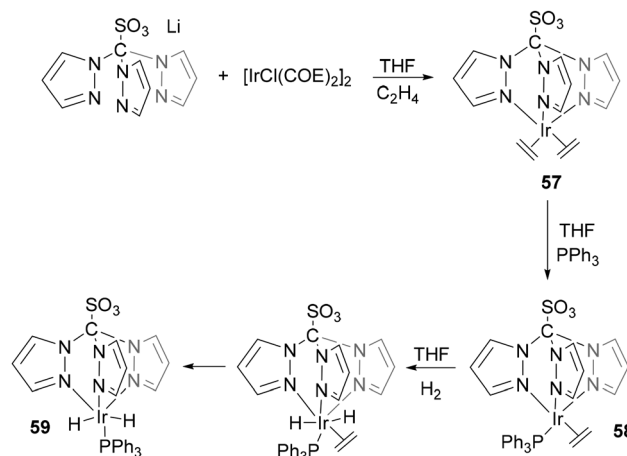


**Scheme 13** Synthesis of rhodium(I) tris(pyrazolyl)methanesulfonate complexes bearing carbonyl and olefin ligands. Reaction of Ti(Tpms) with [Rh(CO)<sub>2</sub>Cl]<sub>2</sub>, [Rh(COD)Cl]<sub>2</sub> or [Rh(NBD)Cl]<sub>2</sub> affords Tpms-supported Rh(I) species displaying flexible coordination behaviour and providing entry points to further organometallic reactivity.



quantitative formation of hydrido-aryl products, while analogous experiments in deuterated solvents demonstrate isotopic scrambling, providing clear evidence for genuine C–H activation pathways rather than simple ligand exchange (Scheme 14a). NMR spectroscopy supports these assignments: in **53**, the hydride appears at  $\delta_{\text{H}} = -16.30$  ppm as a doublet of doublets ( $^1J_{\text{RhH}} = 26.0$  Hz,  $^2J_{\text{PH}} = 32.3$  Hz), consistent with related Cp\* (pentamethylcyclopentadienyl) and Tp\* (tris(3,5-dimethylpyrazolyl)borate) analogues,<sup>43–45</sup> while the corresponding deuteride signal in **54** is observed at  $\delta_{\text{D}} = -16.1$  ppm in the  $^2\text{H}$  NMR spectrum, with coupling constants reduced according to the magnetogyric ratio of deuterium ( $^1J_{\text{RhD}} = 4$  Hz,  $^2J_{\text{PD}} = 5$  Hz). After short irradiation times, NMR analysis also reveals the formation of the carbon monoxide insertion product  $[(\text{TpmsRh}(\text{H})(\text{COC}_6\text{H}_5)(\text{PMe}_3))]$ , identified by its characteristic hydride resonance at  $\delta_{\text{H}} = -14.88$  ppm as a doublet of doublets, confirming the accessibility of benzoyl intermediates under mild photochemical conditions. The incorporation of water-soluble phosphines further extends Tpms–Rh chemistry into polar media. Complexes such as  $[\text{Rh}(\text{Tpms})(\text{CO})(\text{PTA})]$  (**56**) (PTA = 1,3,5-triaza-7-phosphaadamantane) combine  $\kappa^3$ -*N,N,N* scorpionate binding with labile donor environments and exhibit well-defined electrochemical responses, while maintaining sufficient stability for solution studies (Scheme 14b).<sup>46</sup> These systems illustrate how Tpms ligands can balance coordination rigidity with functional adaptability in late-metal organometallic chemistry.

Iridium analogues complete this picture by extending Tpms chemistry to oxidative addition processes. Reaction of  $[\text{IrCl}(\text{COE})_2]_2$  (COE = *cis*-cyclooctene) with  $\text{Li}(\text{Tpms})$  affords ethylene complexes that readily undergo ligand substitution and



**Scheme 15** Ethylene coordination, phosphine substitution and dihydrogen oxidative addition in iridium(i) tris(pyrazolyl)methanesulfonate complexes.

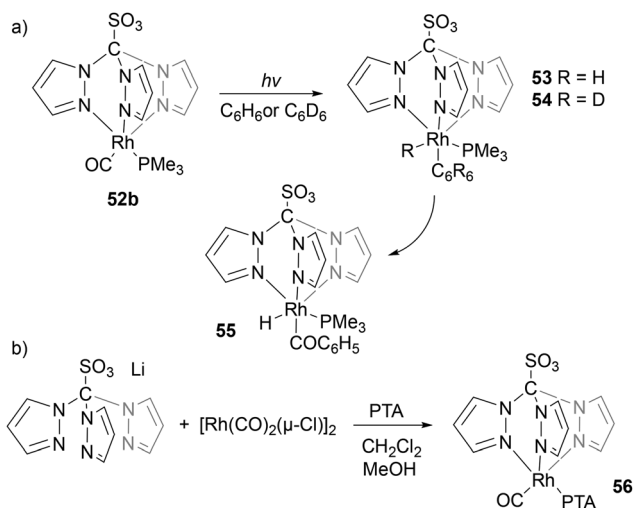
hydrogen activation to form *cis*-dihydride species (Scheme 15).<sup>47</sup> These transformations demonstrate that the sulfonated scorpionate framework can accommodate  $\pi$ -ligand coordination, oxidative addition and metal–hydride formation without loss of structural integrity.

Collectively, the organometallic chemistry of Fe, Ru, Rh and Ir supported by Tpms ligands reveals a coherent picture in which classical scorpionate coordination is retained while access to carbonyls, hydrides,  $\eta^2$ - $\text{H}_2$  complexes, cyanometallate motifs and C–H activation intermediates is enabled. These studies establish Tpms ligands as genuinely enabling platforms for organometallic reactivity, particularly in polar or protic environments where traditional scorpionates are often ineffective.

### 3.5. Coinage metals and structural diversity: discrete complexes, polymers and extended architectures

The coordination chemistry of coinage metals (Cu, Ag and Au) with tris(pyrazolyl)methanesulfonate (Tpms) ligands represents one of the most structurally diverse manifestations of this ligand family, reflecting the combined influence of soft metal centres, hemilabile sulfonate coordination and flexible tripodal nitrogen binding. In contrast to earlier transition-metal systems, Tpms–coinage metal chemistry spans discrete molecular complexes, multinuclear assemblies and extended coordination polymers.

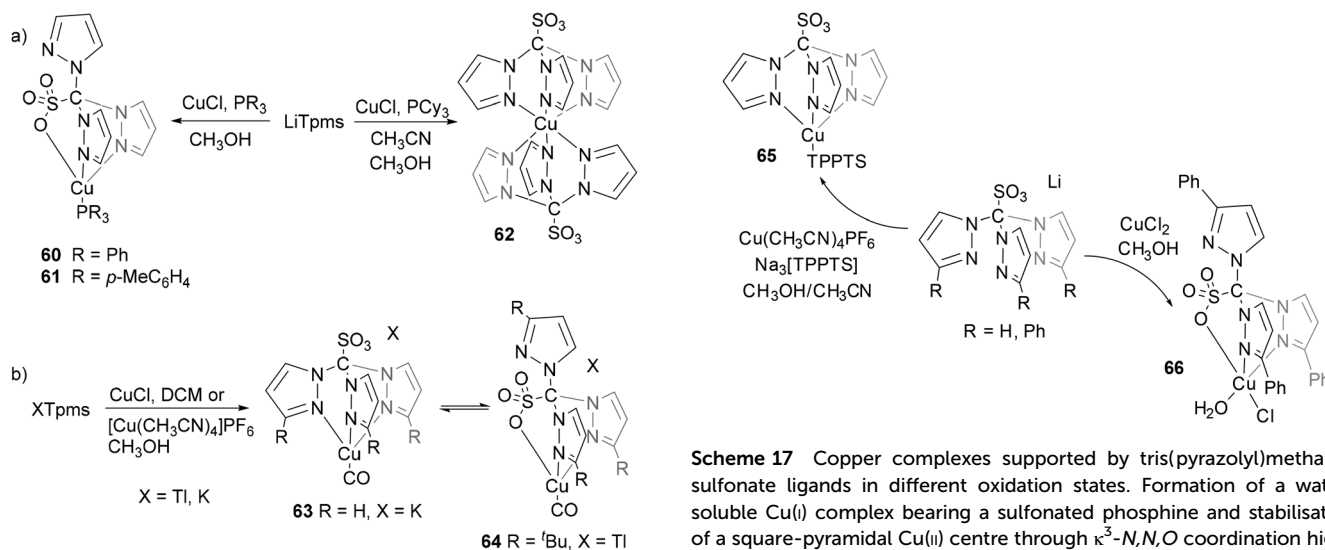
Copper(i) complexes provided the first direct structural evidence of Tpms coordination to coinage metals. Santini and co-workers reported mixed phosphine–Tpms Cu(i) species such as  $[\text{Cu}(\text{PPh}_3)(\text{Tpms})]$  (**60**) and related derivatives, in which Tpms adopts a heteroscorpionate  $\kappa^3$ -*N,N,O* coordination mode, leading to distorted tetrahedral Cu(i) centres (Scheme 16a).<sup>31</sup> In the absence of sterically compatible phosphines, bis-ligand species  $[\text{Cu}(\text{Tpms})_2]$  (**62**) are preferentially formed, highlighting the adaptability of the Tpms donor set. Variable-temperature NMR studies revealed pronounced fluxio-



**Scheme 14** Photochemical and ligand-substitution reactivity of rhodium(i) tris(pyrazolyl)methanesulfonate complexes: (a) Photolysis of carbonyl–phosphine derivatives generates coordinatively unsaturated Rh(i) species that undergo C–H bond activation and CO insertion to form hydrido–aryl and acyl complexes; and (b) Incorporation of water-soluble phosphines such as PTA affords well-defined Rh–Tpms species compatible with polar media.



## Perspective



**Scheme 16** Copper(I) complexes supported by tris(pyrazolyl)methane-sulfonate ligands: (a) The formation of mixed phosphine–Tpms species and bis(Tpms) derivatives illustrates the balance between heteroscorpionate  $\kappa^3$ -*N,N,O* coordination; and (b) fully tripodal  $\kappa^3$ -*N,N,N* binding, as well as the influence of pyrazolyl substitution on Cu(I) coordination environments.

nal behaviour, attributed to rapid pyrazolyl arm exchange and weak Cu–O(sulfonate) interactions.

The donor balance within Tpms was further illustrated by copper(I) carbonyl complexes. Kläui and co-workers compared  $[(\text{Tpms}^{\text{tBu}})\text{Cu}(\text{CO})]$  (**64**) and  $[(\text{Tpms})\text{Cu}(\text{CO})]$  (**63**), demonstrating that steric encumbrance at the pyrazolyl rings favours  $\kappa^3$ -*N,N,O* coordination in Tpms<sup>tBu</sup> derivatives, whereas the less hindered Tpms ligand preferentially adopts a  $\kappa^3$ -*N,N,N* mode (Scheme 16b).<sup>22</sup> Variable-temperature NMR and IR spectroscopy showed that bulky substituents promote a *C*<sub>s</sub>-symmetric *N,N,O* coordination, associated with an intense  $\nu(\text{CO})$  band at 2108 cm<sup>-1</sup>, while non-substituted Tpms favours a *C*<sub>3v</sub>-symmetric isomer with  $\nu(\text{CO}) = 2104$  cm<sup>-1</sup>. These systems underscore how subtle ligand modifications dictate coordination symmetry and electronic properties at soft Cu(I) centres. Copper(II) derivatives extend this chemistry to higher coordination numbers. The square-pyramidal complex  $[\text{CuCl}(\text{Tpms}^{\text{Ph}})(\text{H}_2\text{O})]$  (**66**) illustrates how the sulfonate group can directly participate in metal binding, stabilising  $\kappa^3$ -*N,N,O* coordination modes in Cu(II) environments (Scheme 17).<sup>48</sup> Solid- and solution-state spectroscopic data confirm partial sulfonate engagement, reinforcing the role of Tpms as more than a purely *N*-donor ligand. In parallel, the water-soluble copper(I) complex  $[\text{Cu}(\text{TPPTS})(\text{Tpms})]$  (**65**), obtained from  $[\text{Cu}(\text{CH}_3\text{CN})_4]\text{PF}_6$ ,  $\text{Na}_3[\text{TPPTS}]$  (TPPTS = P(C<sub>6</sub>H<sub>4</sub>-*m*-SO<sub>3</sub>)<sub>3</sub>) and Li(Tpms) in CH<sub>3</sub>OH/CH<sub>3</sub>CN, further demonstrates the compatibility of Tpms-based systems with highly polar and aqueous media (Scheme 17).<sup>49</sup>

Silver(I) systems exhibit the most pronounced structural diversity within coinage-metal Tpms chemistry. Discrete Ag(I) complexes such as  $[\text{Ag}(\text{Tpms})]$  (**67**) exhibit predominantly  $\kappa^3$ -*N*,

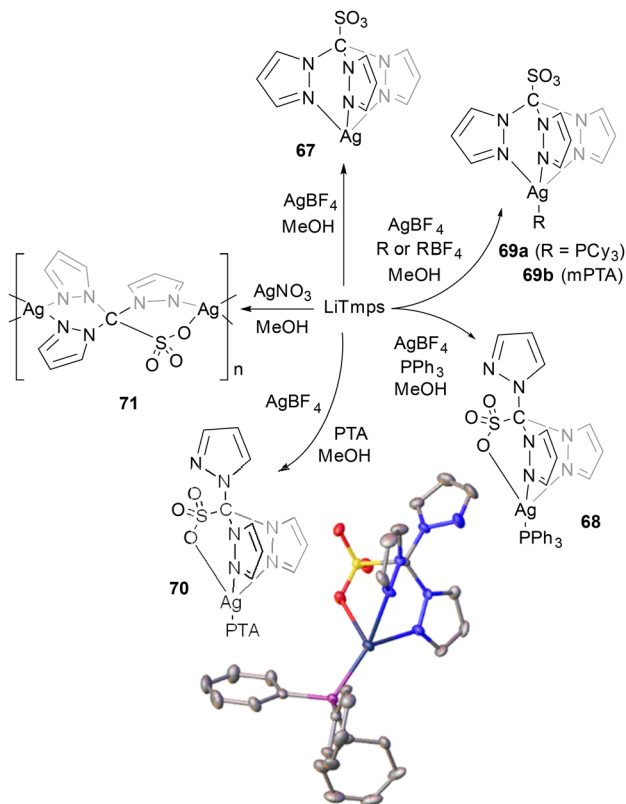
**Scheme 17** Copper complexes supported by tris(pyrazolyl)methane-sulfonate ligands in different oxidation states. Formation of a water-soluble Cu(I) complex bearing a sulfonated phosphine and stabilisation of a square-pyramidal Cu(II) centre through  $\kappa^3$ -*N,N,O* coordination highlight the role of the sulfonate group in enhancing solubility and enabling higher coordination numbers.

*N,N* coordination in solution, but weak Ag...O(sulfonate) interactions can promote oligomerisation or polymerisation in the solid state (Scheme 18).<sup>50</sup> The outcome is highly sensitive to auxiliary ligands: phosphine- and PTA-stabilised complexes remain molecular,<sup>50,51</sup> whereas ligand-only systems readily assemble into extended architectures. A particularly striking example is the one-dimensional helical coordination polymer  $[\text{Ag}(\text{Tpms})]_n$  (**71**), in which Tpms bridges adjacent Ag centres through alternating *N*- and *O*-donor sets (Scheme 18).<sup>52</sup> This structure highlights the ability of Tpms to function simultaneously as a chelating and bridging ligand, enabling polymer formation without additional spacers or multitopic linkers.

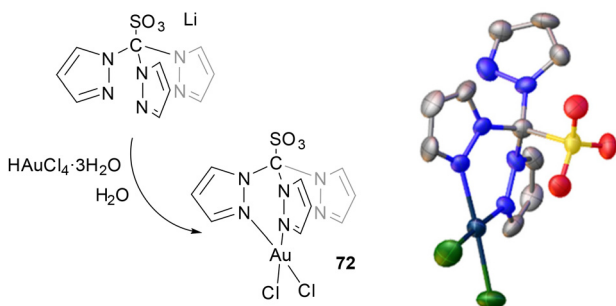
Gold(III) chemistry, though more limited, reinforces the intrinsic donor hierarchy of Tpms ligands. In the square-planar complex  $[\text{AuCl}_2(\text{Tpms})]$  (**72**), Tpms coordinates exclusively through two pyrazolyl nitrogen atoms, leaving both the sulfonate group and one pyrazolyl arm unbound (Scheme 19).<sup>53</sup> NMR studies in DMSO-*d*<sub>6</sub> show rapid exchange among the pyrazolyl arms, whereas X-ray diffraction reveals an almost ideal square-planar Au(III) centre with two chloride ligands and two coordinated pyrazolyl donors. This selective coordination behaviour reflects the preference of Au(III) for soft *N*-donor environments and suggests opportunities for secondary interactions or post-coordination assembly.

Overall, coinage-metal Tpms chemistry showcases the ligand as a genuine structure-directing platform rather than a passive spectator. The interplay between soft metal centres, hemilabile sulfonate coordination and tripodal nitrogen binding enables access to a continuum of nuclearities and dimensionalities—from fluxional mononuclear complexes to discrete Ag(I) assemblies and extended coordination polymers. This structural adaptability clearly distinguishes Tpms from classical scorpionate ligands and underpins its growing relevance in the rational design of functional metal-based architectures.





**Scheme 18** Structural diversity of silver(I) tris(pyrazolyl)methanesulfonate complexes. Modulation of auxiliary ligands and reaction conditions enables access to Ag(I) species, phosphine- or PTA-stabilised complexes, and oligomeric or polymeric assemblies, reflecting the balance between  $\kappa^3$ -*N,N,N* coordination and secondary Ag–O(sulfonate) interactions. The solid-state structure of complex **68**, shown with 50% probability ellipsoids, illustrates a representative coordination environment. Hydrogen atoms are omitted for clarity.



**Scheme 19** Gold(III) tris(pyrazolyl)methanesulfonate complex illustrating selective *N*-donor coordination. The solid-state structure of [AuCl<sub>2</sub>(Tpms)] (**72**) is shown with 50% probability ellipsoids. Hydrogen atoms are omitted for clarity.

### 3.6. Emerging design rules from Tpms-supported metal complexes

The body of work reviewed in this section reveals that tris(pyrazolyl)methanesulfonate ligands are not merely water-compatible analogues of classical scorpionates, but versatile design

elements that enable systematic control over coordination mode, nuclearity and reactivity across a broad range of metal centres. Several general design rules can be distilled from Tpms-supported metal complexes. A first and central feature is the hierarchy and complementarity of donor sites. While the three pyrazolyl nitrogen atoms define a robust facial N<sub>3</sub> platform, the appended sulfonate group introduces an additional, weaker donor that can engage selectively depending on the electronic demands, coordination number and hardness of the metal centre. This hierarchy enables predictable differentiation between fully tripodal  $\kappa^3$ -*N,N,N* coordination, heteroscorpionate  $\kappa^3$ -*N,N,O* binding and lower denticity modes such as  $\kappa^2$ -*N,N*, particularly in metals capable of accommodating higher coordination numbers or secondary interactions. Closely related to this is the hemilabile character of the sulfonate group, which allows reversible engagement without compromising the integrity of the tripodal scaffold. Across multiple metal families, sulfonate coordination emerges as a responsive element rather than a fixed binding site, adapting to changes in oxidation state, solvent polarity or the presence of auxiliary ligands. This behaviour underpins dynamic processes such as coordination switching, fluxionality in solution and the stabilisation of reactive intermediates, while maintaining high hydrolytic stability. A third recurring design principle is the control of nuclearity and dimensionality. Tpms ligands can stabilise well-defined mononuclear complexes, but they also readily support multinuclear assemblies and extended architectures when secondary metal–sulfonate or metal–metal interactions become energetically favourable. In particular, coinage-metal systems highlight how subtle changes in ligand environment or reaction conditions can shift the outcome from discrete species to coordination polymers, without the need for multitopic or rigid organic linkers. The reviewed examples further demonstrate that steric modulation at the pyrazolyl rings provides an efficient handle to fine-tune coordination symmetry and electronic properties. Bulky substituents favour reduced denticity or heteroscorpionate binding, whereas less hindered systems promote fully tripodal coordination. This steric control directly translates into changes in metal geometry, ligand lability and reactivity, offering a modular strategy for catalyst and material design.

Finally, Tpms ligands combine structural robustness with functional adaptability, particularly under polar or aqueous conditions. The sulfonate group enhances solubility and stability without sacrificing coordination versatility, positioning Tpms as a powerful scaffold for sustainable inorganic chemistry. Importantly, the ligand framework supports a wide range of oxidation states and metal classes, from early transition metals to coinage and post-transition metals, enabling the transfer of design principles between traditionally distinct areas of inorganic chemistry.

## 4. Applications

### 4.1. Antimicrobial and antiproliferative activities

The biological applications of Tpms-based metal complexes have been widely explored over the past two decades, particu-



larly for copper(i) and silver(i) derivatives. In 2003, Santini and co-workers investigated the antioxidant activity of the copper(i) complex  $[\text{Cu}[\text{PPh}_2(p\text{-C}_6\text{H}_4\text{COOH})]_2(\text{Tpms})]$  using lucigenin-enhanced chemiluminescence, a technique that selectively detects free superoxide radicals not quenched by antioxidants.<sup>54</sup> This complex efficiently scavenged superoxide anions, showing an  $\text{IC}_{50}$  value of  $0.57 \pm 0.06$  mM. The activity was attributed to the electron-donating properties of the scorpionate ligand, which were proposed to enhance the complex's reactivity toward reactive oxygen species. Pellei and co-workers (2004) extended these studies to the copper(i) derivative  $[\text{CuTpms}(\text{TPPTS})]$  (**65**), also assessed by lucigenin chemiluminescence.<sup>49</sup> While complex **65** exhibited the highest antioxidant performance, its capacity to prevent DNA strand breakage depended strongly on the reactive nitrogen–oxygen species donor used. Notably, complex **65** significantly protected DNA only in the presence of the SIN-1 donor, highlighting a selective protective effect against specific sources of oxidative stress.

The biological scope of Tpms complexes was later expanded to silver derivatives. Pettinari and co-workers (2011) evaluated the antimicrobial properties of  $[\text{Ag}(\text{Tpms})]$  (**67**)– $[\text{Ag}(\text{PTA})(\text{Tpms})]$  (**70**) by agar diffusion assays against a panel of bacteria and fungi.<sup>50</sup> While the lithium salt of Tpms alone was inactive, all silver complexes displayed broad-spectrum antibacterial and antifungal activity. The PTA-containing complex **70** was particularly potent, showing significantly greater antibacterial activity than silver nitrate ( $P < 0.01$ ). It inhibited both Gram-positive and Gram-negative strains, except *Enterococcus faecalis*, known for its high intrinsic tolerance, and demonstrated strong activity against *Pseudomonas aeruginosa* as well as excellent antifungal effects against *Candida albicans* (inhibition zones  $\approx 20$  mm). These results underscore the potential of silver(i) Tpms complexes, especially PTA-containing derivatives, as potent antimicrobial agents.

Continuing the exploration of silver-based systems, Almeida and co-workers (2019) investigated the antiproliferative properties of the coordination polymer  $[\text{Ag}(\text{Tpms})]_n$  (**71**) using MTS assays on ovarian carcinoma (A2780) and colorectal carcinoma (HCT116) cell lines.<sup>52</sup> The polymer showed marked, concentration-dependent cytotoxicity with striking selectivity toward A2780, achieving an exceptionally low  $\text{IC}_{50}$  of  $0.04$   $\mu\text{M}$  (vs.  $4.73$   $\mu\text{M}$  for HCT116). Notably, the effect on non-tumor fibroblasts resembled that observed for HCT116, suggesting a promising therapeutic window for selectively targeting ovarian carcinoma. Mechanistic studies indicated rapid disruption of A2780 cell adherence, likely driven by controlled  $\text{Ag}^+$  release, and apoptosis as the main cell death pathway. These findings highlight Tpms-based silver(i) coordination polymers as promising candidates for anticancer therapy.

The antimicrobial potential of silver(i) Tpms systems was further examined by Smolenski and co-workers (2015), who studied  $[\text{Ag}(\text{mPTA})_4](\text{Tpms})_4(\text{BF}_4)$  and  $[\text{Ag}(\text{Tpms})(\text{mPTA})]$  (**69b**) against pathogenic bacteria and fungi using the microdilution method.<sup>51</sup> The former consistently exhibited lower MIC values (8–128  $\mu\text{M}$ ) than compound **69b** (32–256  $\mu\text{M}$ ), particularly against Gram-negative bacteria (*E. coli*, *P. aeruginosa*) and

*Candida albicans* (8–32  $\mu\text{M}$ ). Both complexes were less active against Gram-positive species, showing mainly bacteriostatic effects. Importantly, compound  $[\text{Ag}(\text{mPTA})_4](\text{Tpms})_4(\text{BF}_4)$  retained the antibacterial potency of  $\text{AgNO}_3$ , while the structure of **69b** appeared to reduce silver bioavailability and activity. The presence of hydrophobic ligands in both complexes was suggested to facilitate interactions with microbial membranes, enhancing silver ion action. In addition, their interaction with thiol-rich proteins was probed using adenosine deaminase (ADA) as a model enzyme: unlike  $\text{AgNO}_3$ , which competitively inhibits ADA *via* cysteine binding, neither complex significantly interfered with enzyme activity. This selectivity suggests the potential for antimicrobial efficacy combined with reduced off-target protein reactivity.

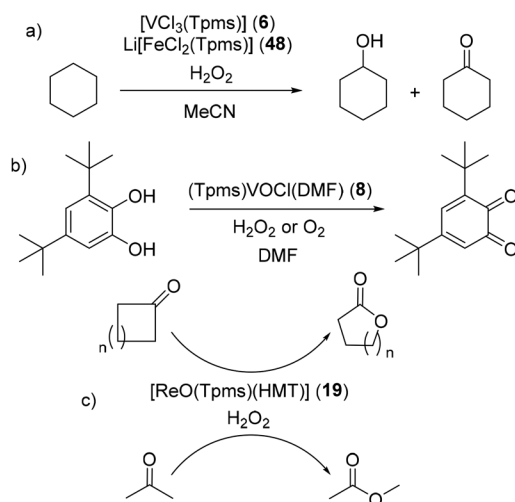
#### 4.2. Catalytic functions

The versatile coordination properties of the tris(pyrazolyl)methanesulfonate (Tpms) ligand and its derivatives have enabled the development of a wide range of catalytic systems spanning early and late transition metals. The combination of electronic tunability, hemilabile coordination and variable denticity allows Tpms-based complexes to participate in diverse transformations, including oxidations, carbonylations, and C–C bond-forming reactions, often under mild and sustainable conditions.

Vanadium complexes were among the earliest Tpms-based catalysts to be explored. A particularly well-studied transformation is the oxidation of cyclohexane, where Tpms-based complexes serve as effective catalysts under environmentally benign conditions. Silva *et al.* demonstrated that vanadium, iron, and copper complexes synthesized from the reaction between the corresponding chlorides in alcohol solvents, in the presence of  $\text{LiTpms}$ , catalyse the single-pot oxidation of cyclohexane to cyclohexanol and cyclohexanone using  $\text{H}_2\text{O}_2$  as an environmentally friendly oxidant (Scheme 20a).<sup>18</sup> Among these, the iron complex  $\text{Li}[\text{FeCl}_2(\text{Tpms})]$  (**48**) demonstrated the highest activity promoted by the use of acid, operating efficiently in aqueous media without the need for organic solvents, owing to its high solubility. Mechanistic studies pointed to a radical pathway, likely involving C- and O-centered radicals in conjunction with a metal-based oxidant. Building on this work, Mishra *et al.* explored the vanadium(III) complex  $[\text{VCl}_3(\text{Tpms})]$  (**6**) as a catalyst precursor for the selective oxidation of cyclohexane with dioxygen in a one-pot, solvent-free process.<sup>55</sup> Optimal activity was achieved at  $140$   $^\circ\text{C}$ ,  $15$  atm  $\text{O}_2$ , and  $18$  h, with pyridine-2-carboxylic acid (PCA) significantly boosting performance, underscoring the versatility of Tpms-supported vanadium complexes in oxidative catalysis.

Following these studies on chlorinated vanadium complexes,<sup>18,55</sup> the catalytic activity of the oxovanadium complexes was also investigated. The complex  $(\text{Tpms})\text{VOCl}(\text{DMF})$  (**8**) catalyses the oxidation of 3,5-di-*tert*-butyl catechol to the corresponding quinone with  $\text{H}_2\text{O}_2$  in DMF, achieving on average 65% conversion under optimized conditions, with the remaining 35% corresponding to other oxidation products (Scheme 20b).<sup>56</sup>





**Scheme 20** Representative catalytic transformations promoted by Tpms-based complexes. (a) Oxidation of cyclohexane to cyclohexanol and cyclohexanone using  $\text{H}_2\text{O}_2$  as the oxidant; (b) oxidation of 3,5-di-*tert*-butylcatechol to the corresponding quinone catalysed by an oxovanadium complex; and (c) Baeyer–Villiger oxidation of ketones to esters or lactones mediated by a rhenium complex.

Further studies showed that the vanadium(v) complex  $[\text{VO}_2(\text{Tpms})]$  (**9**) is highly effective in the carboxylation of methane and ethane, reaching yields of up to 40%, and outperforming analogous systems containing neutral scorpionates such as hydrotris(1-pyrazolyl)methane.<sup>36</sup>

This complex also catalyses the oxidation of cycloalkanes (cyclohexane and cyclopentane) with aqueous  $\text{H}_2\text{O}_2$ , selectively affording alcohols and ketones. The catalytic performance is comparable to that of the previously reported chloro-V(IV) compounds (**6**),<sup>18</sup> reaching turnover numbers (TONs) of 117 and 120 when complexes **6** and **9** were used, respectively. These results underscore the ability of Tpms ligands to stabilize vanadium centers in high-oxidation-state processes.

The catalytic scope of Tpms extends to other early transition metals. The rhenium(III) complex  $[\text{ReO}(\text{Tpms})(\text{HMT})]$  (**19**) mediates Baeyer–Villiger oxidations of cyclic and acyclic ketones with  $\text{H}_2\text{O}_2$  as the oxidant under mild conditions (70 °C, 6 h in dichloroethane) in a one-pot process.<sup>28</sup> High turnover numbers (TONs) are observed, particularly for small-ring ketones such as cyclobutanone, and substrates like 2-methylcyclohexanone and pinacolone are efficiently converted to lactones and esters (Scheme 20c). The Tpms ligand plays a key role in stabilising reactive oxygenated intermediates, facilitating selective oxygen insertion.

In contrast, ruthenium systems have shown more limited performance. Complexes such as  $[\text{Ru}(p\text{-cymene})(\text{Tpms})]\text{Cl}$  (**24**) and  $[\text{Ru}(p\text{-cymene})(\text{Tpms}^{\text{Ph}})]\text{Cl}$  (**27**) catalyse the oxidation of styrene with  $\text{H}_2\text{O}_2$  in acetone (1 mol% loading), but only benzaldehyde is detected in modest yield (~20%), and even increasing the catalyst concentration leads to only moderate improvements.<sup>23</sup>

Tpms-based rhodium complexes offer a notable exception among late transition metals. The complex  $[(\text{Tpms})\text{Rh}(\text{CO})$

$(\text{PMe}_3)]$  (**52b**) is the only known tripodal-ligand catalyst capable of promoting benzene carbonylation.<sup>42</sup> Its relatively low steric hindrance and the push–pull electronic effect of Tpms and  $\text{PMe}_3$  maintain metal-center accessibility while stabilizing both Rh(I) and Rh(III) intermediates. This enables the isolation of rare catalytic species such as the hydridophenyl  $[(\text{Tpms})\text{Rh}(\text{H})(\text{C}_6\text{H}_5)(\text{PMe}_3)]$  (**53**) and hydridobenzoyl  $[(\text{Tpms})\text{Rh}(\text{H})(\text{COC}_6\text{H}_5)(\text{PMe}_3)]$  (**55**) complexes, which are typically difficult to trap in related systems. Later, the use of  $\text{TpmsRh}(\text{CO})_2$  (**51**) in the hydroformylation of 1-hexene was studied.<sup>57</sup> The reaction takes place under mild conditions and in the absence of added phosphines such as the previously reported catalyst used in the carbonylation of benzene.<sup>42</sup> The catalyst exhibits high selectivity for the linear aldehyde, whereas the analogous complex  $\text{Tp}^*\text{Rh}(\text{CO})_2$  preferentially forms the branched aldehyde. During catalysis, a bis(acyl) rhodium(III) complex is formed.

The  $[\text{Ir}(\text{Tpms})(\text{H})_2(\text{PPh}_3)]$  (**59**) complex was tested in the hydrogenation of the sterically hindered 3,3-dimethyl-1-butene, achieving complete conversion to the desired 2,2-dimethylbutane.<sup>47</sup> Notably, increasing the  $\text{H}_2$  pressure from 1 to 2 atm using a Parr hydrogenator resulted in a shorter reaction time, underscoring the beneficial effect of higher hydrogen pressure on the catalytic performance.

Tpms derivatives have also shown promise in Lewis acid catalysis. The phenyl derivatives  $[\text{NiCl}(\text{Tpms}^{\text{Ph}})]$  (**2**),  $[\text{ZnCl}(\text{Tpms}^{\text{Ph}})]$  (**1a**), and  $[\text{CuCl}(\text{Tpms}^{\text{Ph}})(\text{H}_2\text{O})]$  (**66**) were tested in the Henry (nitroaldol) reaction of benzaldehyde with nitroethane in methanol.<sup>48</sup> While the nickel complex showed low activity, the zinc(II) and copper(II) species efficiently catalysed the reaction, reaching yields of up to 99% at room temperature with a predominance of the *anti* diastereoisomer. Notably, the zinc complex exhibited the best diastereoselectivity, with *anti/syn* ratios up to 2.3. Mechanistic insights suggest that the metal center acts as a Lewis acid to activate the aldehyde and nitroethane, while the  $\text{Tpms}^{\text{Ph}}$  ligand behaves as a Brønsted base, assisting nitronate formation.

The newly described gold(III) compound  $[\text{AuCl}_2(\text{Tpms})]$  (**72**) was tested<sup>53</sup> for the first time in the oxidation of toluene and benzyl alcohol. Maximum yields of 8% were achieved for toluene oxidation, affording benzyl alcohol and benzaldehyde, while benzyl alcohol oxidation reached a 35% yield, producing benzaldehyde with 75% selectivity relative to benzoic acid. In both reactions, mild conditions were employed, with reaction times not exceeding 24 hours. Furthermore, the oxidative esterification of benzaldehyde to form methyl benzoate was carried out under similarly mild conditions, yielding encouraging conversions and selectivities.

Taken together, these studies reveal the broad catalytic versatility of Tpms-based systems, from vanadium-mediated oxidations and rhenium-catalysed Baeyer–Villiger reactions to rhodium-promoted carbonylations, Lewis acid-driven C–C bond formation, and the selective peroxidative oxidation of alkanes. The balance of electronic donation, multi-dentate coordination, and the capacity to stabilize diverse metal oxidation states makes Tpms a privileged scaffold for the development of efficient and sustainable catalysts.



## 5. Conclusions and outlook

Tris(pyrazolyl)methanesulfonate ligands have evolved from simple sulfonated analogues of classical scorpionates into versatile and functionally rich platforms for modern inorganic chemistry. The body of work discussed in this Perspective demonstrates that Tpms ligands uniquely integrate facial *N,N,N* coordination, enhanced solubility in polar and aqueous media, and a tunable sulfonate functionality within a single, robust scaffold. This combination enables systematic control over coordination mode, nuclearity and the metal-centre environment across a wide range of elements and oxidation states.

A defining feature of Tpms chemistry is the hierarchical organisation of donor sites, in which strong pyrazolyl nitrogen coordination is complemented by a weaker, adaptable sulfonate interaction. This donor complementarity accounts for the remarkable structural diversity observed, from well-defined mononuclear complexes to multinuclear assemblies and extended coordination polymers. Importantly, the sulfonate group operates as a responsive structural element rather than a passive substituent, allowing reversible engagement without compromising hydrolytic stability or ligand integrity. These structural attributes translate directly into functional behaviour. Tpms-supported complexes have demonstrated activity in oxidation, carbonylation and C–C bond-forming catalysis, often under mild and environmentally compatible conditions, while silver- and copper-based systems exhibit promising antimicrobial and antiproliferative properties. In both contexts, the balance between ligand rigidity and adaptability appears critical, enabling stabilisation of reactive intermediates, modulation of metal accessibility and, in some cases, controlled metal-ion release.

Looking forward, several opportunities and challenges can be identified. Greater mechanistic insight, particularly under aqueous or biologically relevant conditions, will be essential to move Tpms-based systems beyond proof-of-concept studies. Rational ligand design, including targeted substitution at the pyrazolyl rings or controlled modification of the sulfonate environment, offers a clear pathway to fine-tune steric and electronic effects and to direct nuclearity or dimensionality. In catalysis, benchmarking against established ligand classes under comparable conditions will be crucial to define the true advantages of Tpms frameworks. In biologically related applications, understanding structure–activity relationships and metal release pathways will be key to improving selectivity and reducing off-target effects.

Continued exploration of this ligand family is therefore expected to yield not only new structures but also deeper insight into how multifunctional ligand architectures can be exploited in contemporary inorganic chemistry.

## Author contributions

Arantxa Forte-Castro: investigation and writing – original draft.  
Juana M. Pérez: investigation, validation, and writing – original

draft. Ignacio Fernández: conceptualization, funding acquisition, project administration, supervision, validation, visualization, and writing – review & editing.

## Conflicts of interest

The authors declare no conflict of interest.

## Data availability

No primary research results, software or code have been included, and no new data were generated or analysed as part of this Perspective. All the information and data presented have been taken from the cited references.

## Acknowledgements

This research has been funded by the State Research Agency of the Spanish Ministry of Science, Innovation and Universities (PID2021-126445OB-I00 and PID2023-150047OA-I00) by the Spanish Government MCIU/AEI/10.13039/501100011033/FEDER, EU, by the European Union “Next Generation EU”/PRTR and Junta de Andalucía (P20\_01041). J. M. P. acknowledges the Spanish Investigation Agency and the Ministry of Science, Innovation and Universities for the Ramon y Cajal fellowship (RYC2024-048173-I).

## References

- 1 J. M. Smith, *Comments Inorg. Chem.*, 2008, **29**, 189–233.
- 2 S. Trofimenko, *Scorpionates: The Coordination Chemistry Of Polypyrazolylborate Ligands*, London, 1999.
- 3 H. V. Rasika Dias and T. K. H. H. Goh, *Polyhedron*, 2004, **23**, 273–282.
- 4 S. Trofimenko, *J. Am. Chem. Soc.*, 1967, **89**, 3165–3170.
- 5 H. De Bari and M. Zimmer, *Inorg. Chem.*, 2004, **43**, 3344–3348.
- 6 S. Trofimenko, *Chem. Rev.*, 1993, **93**, 943–980.
- 7 H. V. Rasika Dias and S. A. Polach, *Inorg. Chem.*, 2000, **39**, 4676–4677.
- 8 D. Buccella, A. Shultz, J. G. Melnick, F. Konopka and G. Parkin, *Organometallics*, 2006, **25**, 5496–5499.
- 9 X. Hu and K. Meyer, *J. Organomet. Chem.*, 2005, **690**, 5474–5484.
- 10 A. Paulo, J. D. G. Correia, M. P. C. Campello and I. Santos, *Polyhedron*, 2004, **23**, 331–360.
- 11 S. Trofimenko, *Acc. Chem. Res.*, 1971, **4**, 17–22.
- 12 H. R. Bigmore, S. C. Lawrence, P. Mountford and C. S. Tredget, *Dalton Trans.*, 2005, 635–651.
- 13 C. Pettinari and R. Pettinari, *Coord. Chem. Rev.*, 2005, **249**, 663–691.
- 14 R. Garcia, A. Paulo and I. Santos, *Inorg. Chim. Acta*, 2009, **362**, 4315–4327.



- 15 C. Pettinari and C. Santini, in *Comprehensive Coordination Chemistry II*, Elsevier, 2003, pp. 159–210.
- 16 M. Kosugi, S. Hikichi, M. Akita and Y. Moro-oka, *Inorg. Chem.*, 1999, **38**, 2567–2578.
- 17 E. Kime-Hunt, K. Spartalian, M. DeRusha, C. M. Nunn and C. J. Carrano, *Inorg. Chem.*, 1989, **28**, 4392–4399.
- 18 T. F. S. Silva, E. C. B. A. Alegria, L. M. D. R. S. Martins and A. J. L. Pombeiro, *Adv. Synth. Catal.*, 2008, **350**, 706–716.
- 19 J. M. Muñoz-Molina, T. R. Belderrain and P. J. Pérez, *Dalton Trans.*, 2019, **48**, 10772–10781.
- 20 W. Kläui, M. Berghahn, G. Rheinwald and H. Lang, *Angew. Chem., Int. Ed.*, 2000, **39**, 2464–2466.
- 21 S. Miguel, J. Diez, M. P. Gamasa and M. E. Lastra, *Eur. J. Inorg. Chem.*, 2011, 4745–4755.
- 22 W. Kläui, M. Berghahn, W. Frank, G. J. Reiß, T. Schönherr, G. Rheinwald and H. Lang, *Eur. J. Inorg. Chem.*, 2003, 2059–2070.
- 23 F. Marchetti, C. Pettinari, R. Pettinari, A. Cerquetella, L. M. D. R. S. Martins, M. F. C. G. Da Silva, T. F. S. Silva and A. J. L. Pombeiro, *Organometallics*, 2011, **30**, 6180–6188.
- 24 L. M. D. R. S. Martins and A. J. L. Pombeiro, *Eur. J. Inorg. Chem.*, 2016, **2016**, 2236–2252.
- 25 W. Kläui, D. Schramm, W. Peters, G. Rheinwald and H. Lang, *Eur. J. Inorg. Chem.*, 2001, 1415–1424.
- 26 E. T. Papish, M. T. Taylor, F. E. Jernigan, M. J. Rodig, R. R. Shawhan, G. P. A. Yap and F. A. Jové, *Inorg. Chem.*, 2006, **45**, 2242–2250.
- 27 T. B. Chenskaya, M. Berghahn, P. C. Kunz, W. Frank and W. Kläui, *J. Mol. Struct.*, 2007, **829**, 135–148.
- 28 L. M. D. R. S. Martins, E. C. B. A. Alegria, P. Smoleński, M. L. Kuznetsov and A. J. L. Pombeiro, *Inorg. Chem.*, 2013, **52**, 4534–4546.
- 29 R. Wanke, P. Smoleński, M. F. C. Guedes Da Silva, L. M. D. R. S. Martins and A. J. L. Pombeiro, *Inorg. Chem.*, 2008, **47**, 10158–10168.
- 30 R. S. Herrick, T. J. Bruncker, C. Maus, K. Crandall, A. Cetin and C. J. Ziegler, *Chem. Commun.*, 2006, **3**, 4330–4331.
- 31 C. Santini, M. Pellei, G. G. Lobbia, A. Cingolani, R. Spagna and M. Camalli, *Inorg. Chem. Commun.*, 2002, **5**, 430–433.
- 32 L. M. R. Jensen, B. F. Abrahams and C. G. Young, *J. Coord. Chem.*, 2013, **66**, 1252–1263.
- 33 T. F. S. Silva, L. M. D. R. S. Martins, M. F. C. Guedes Da Silva, A. R. Fernandes, A. Silva, P. M. Borrallho, S. Santos, C. M. P. Rodrigues and A. J. L. Pombeiro, *Dalton Trans.*, 2012, **41**, 12888–12897.
- 34 T. F. S. Silva, L. M. D. R. S. Martins and A. J. L. Pombeiro, *Port. Electrochim. Acta*, 2006, **24**, 257–259.
- 35 C. C. McLauchlan, M. P. Weberski and B. A. Greiner, *Inorg. Chim. Acta*, 2009, **362**, 2662–2666.
- 36 T. F. S. Silva, K. V. Luzyanin, M. V. Kirillova, M. F. C. Guedes Da Silva, L. M. D. R. S. Martins and A. J. L. Pombeiro, *Adv. Synth. Catal.*, 2010, **352**, 171–187.
- 37 C. Dinoi, M. F. C. Guedes da Silva, E. C. B. A. Alegria, P. Smoleński, L. M. D. R. S. Martins, R. Poli and A. J. L. Pombeiro, *Eur. J. Inorg. Chem.*, 2010, **2010**, 2415–2424.
- 38 E. C. B. Alegria, L. M. D. R. S. Martins, M. Haukka and A. J. L. Pombeiro, *Dalton Trans.*, 2006, 4954–4961.
- 39 D. V. Fomitchev, C. C. McLauchlan and R. H. Holm, *Inorg. Chem.*, 2002, **41**, 958–966.
- 40 K. S. Naidu and B. R. Jagirdar, *J. Organomet. Chem.*, 2014, **762**, 9–18.
- 41 Z. G. Gu, J. L. Zuo, Y. Song, C. H. Li, Y. Z. Li and X. Z. You, *Inorg. Chim. Acta*, 2005, **358**, 4057–4061.
- 42 W. Kläui, D. Schramm and W. Peters, *Eur. J. Inorg. Chem.*, 2001, 3113–3117.
- 43 W. D. Jones and V. L. Kuykendall, *Inorg. Chem.*, 1991, **30**, 2615–2622.
- 44 W. D. Jones and E. T. Hessell, *J. Am. Chem. Soc.*, 1992, **114**, 6087–6095.
- 45 M. Paneque, P. J. Pérez, A. Pizzano, M. L. Poveda, S. Taboada, M. Trujillo and E. Carmona, *Organometallics*, 1999, **18**, 4304–4310.
- 46 P. Smoleński, C. Dinoi, M. F. C. Guedes da Silva and A. J. L. Pombeiro, *J. Organomet. Chem.*, 2008, **693**, 2338–2344.
- 47 C. M. Nagaraja, M. Nethaji and B. R. Jagirdar, *Organometallics*, 2007, **26**, 6307–6311.
- 48 B. G. M. Rocha, T. C. O. Mac Leod, M. F. C. Guedes da Silva, K. V. Luzyanin, L. M. D. R. S. Martins and A. J. L. Pombeiro, *J. Chem. Soc., Dalton Trans.*, 2014, **43**, 15192–15200.
- 49 M. Pellei, G. G. Lobbia, C. Santini, R. Spagna, M. Camalli, D. Fedeli and G. Falcioni, *Dalton Trans.*, 2004, 2822–2828.
- 50 C. Pettinari, F. Marchetti, G. Lupidi, L. Quassinti, M. Bramucci, D. Petrelli, L. A. Vitali, M. F. C. G. Da Silva, L. M. D. R. S. Martins, P. Smoleński and A. J. L. Pombeiro, *Inorg. Chem.*, 2011, **50**, 11173–11183.
- 51 P. Smoleński, C. Pettinari, F. Marchetti, M. F. C. Guedes da Silva, G. Lupidi, G. V. Badillo Patzmay, D. Petrelli, L. A. Vitali and A. J. L. Pombeiro, *Inorg. Chem.*, 2015, **54**, 434–440.
- 52 J. Almeida, C. Roma-Rodrigues, A. G. Mahmoud, M. F. C. Guedes da Silva, A. J. L. Pombeiro, L. M. D. R. S. Martins, P. V. Baptista and A. R. Fernandes, *J. Inorg. Biochem.*, 2019, **199**, 110789.
- 53 H. M. Lapa, M. F. C. Guedes da Silva, A. J. L. Pombeiro, E. C. B. A. Alegria and L. M. D. R. S. Martins, *Inorg. Chim. Acta*, 2020, **512**, 119881.
- 54 C. Santini, M. Pellei, G. G. Lobbia, D. Fedeli and G. Falcioni, *J. Inorg. Biochem.*, 2003, **94**, 348–354.
- 55 G. S. Mishra, T. F. S. Silva, L. M. D. R. S. Martins and A. J. L. Pombeiro, *Pure Appl. Chem.*, 2009, **81**, 1217–1227.
- 56 C. C. McLauchlan, M. P. Weberski and B. A. Greiner, *Inorg. Chim. Acta*, 2009, **362**, 2662–2666.
- 57 W. Kläui, D. Schramm and G. Schramm, *Inorg. Chim. Acta*, 2004, **357**, 1642–1648.

